

EXPLOITATION OF OPTIMIZATION SOLUTION FOR DETERMINATION OF WHIRL FLUTTER STABILITY BOUNDARIES

Jiri Ceerdle, Ph.D.*

***Aeronautical Research and Test Institute (VZLU), Prague, Czech Republic;
tel.: (+420) 225 115 123; e-mail: ceerdle@vzlu.cz**

Keywords: *aeroelasticity, flutter, whirl flutter*

Abstract

The submitted paper deals with the aircraft structure whirl flutter analysis. It gives a summary of the regulations requirements, the theoretical background and the aircraft certification relating issues. The main part deals with determination of critical engine suspension stiffness parameters considering the structure whirl flutter stability at the certification speed. The optimization-based analytical procedure is demonstrated on the two examples. Finally, the future exploitation of the method is outlined.

1 Introduction

The turboprop aircraft are required to be certified considering the whirl flutter. Rotating parts like a propeller or a turbine increase the number of degrees of freedom and cause additional forces and moments. Moreover rotating propeller causes a complicated flow field and interference effects between wing, nacelle and propeller. Whirl flutter may cause the propeller mounting unstable vibrations, even a failure of the engine, nacelle or whole wing. It has been the cause of a number of accidents (two Lockheed Electra II airliners in 1959 and 1960 and a Beech 1900C commuter in 1991).

At the VZLU, the first tasks regarding the whirl flutter were dealt with in connection with the certification of the Ae-270 small single-engine turboprop aircraft for 8 passengers. Calculations were performed using the model of the cantilevered engine bed with flexibly suspended engine – propeller system [6], [8].

The analysis included just engine vertical and lateral vibration modes, it didn't take under consideration the dynamic characteristics of the residual structure. For the nose-mounted single-engine aircraft, such simplification was acceptable. However the analysis of the classical twin wing-mounted turboprop structure demands to include the residual structure, particularly wing dynamic characteristics and specific aerodynamic propeller – nacelle – wing interference effects. Therefore the analysis procedure was enlarged and adapted also for such configuration. It was demonstrated on the example of commuter aircraft for 40 passengers wing – engine component [7], [8].

2 Motivation

Development of a new aircraft can be divided into following phases: conceptual design, virtual prototype, manufacturing of physical prototype and physical prototype testing.

During the conceptual design phase, the main geometric, aerodynamic, inertia or performance characteristics are estimated. Also the engine – propeller system is chosen, therefore the inertia characteristics of these parts should be known. During the virtual prototype phase, the maximum feasible amount of analyses should be performed, since the virtual structure can be easily refined considering various analyses results. During the next two phases, analyses are kept on. Prototypes are tested; analytical models are improved and updated according the test results etc. Structure

can be also adjusted considering tests or refined analyses results, however, it is obvious, that there are much more limitations or boundary conditions contrary to the previous phase.

Aeroelastic analyses during the first and second phase have mostly overall character to determine possibly critical areas. Number of parameters isn't set with the sufficient level of probability. The final aeroelastic analyses are usually performed after the ground vibration tests of the prototype, when it is possible to update and verify computational models with a satisfactory level of assurance. Obviously, in this phase, analyses have more or less a checking character. Also relatively short period among ground vibration tests and flight flutter tests should be taken under consideration. Therefore, there are efforts to move aeroelastic analyses to the earlier phases. It would allow the structure corrections to prevent possible aeroelastic problems and also timesaving in the later development phases is important. After the ground vibration tests, just checks of the selected critical areas would be performed. Aeroelastic analyses at the virtual prototype phase assume usage of simple and fast tools, good estimation of parameters, automated parametric studies etc. Also the determination of parameter critical values is the acceptable approach.

The most critical parameters influencing the whirl flutter stability are natural frequencies of the flexibly attached engine – propeller system vibrations (vertical and lateral). Airworthiness regulations directly require inclusion of the changes in the stiffness and damping of the propeller – engine – nacelle – structure system (e.g. FAR §23.629(e)(1)(2)). The reliable values of mentioned frequencies aren't at disposal until the ground vibration tests. Assuming the inertia characteristics of the engine – propeller system as reliably determined, the critical parameters are stiffness of the engine system attachment (engine bed, engine mount isolators).

Determination of the critical values, it means the values when the whirl flutter speed is equal to the certification speed would allow replacing large parametric studies varying the stiffness. It would considerably decrease number of

necessary analyses, particularly for the twin wing-mounted engine aircraft, when the number of secondary parameters, like wing inertia and stiffness must be also included. Obviously, it would allow moving the whirl flutter analysis to the early phase of the aircraft development. After the ground vibration tests, just rate of a reserve towards the critical values would be evaluated.

The main aim of the presented paper is a development of such analytical procedure. The optimization – based solution is employed.

3 Theoretical Background

Engine flexible mounting is represented by two rotational springs (stiffness K_ψ , K_θ) as illustrated in fig.1. Propeller is considered as rigid; rotating with angular velocity Ω . System is in the airflow of velocity V_∞ [3], [4].

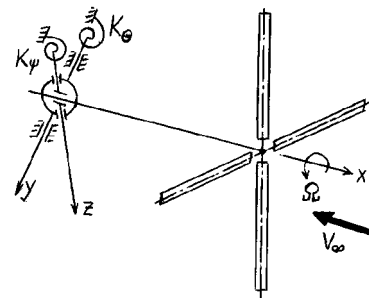


Fig.1. Gyroscopic system with propeller

Neglecting propeller rotation and the aerodynamic forces, the two independent mode shapes (yaw – around vertical axis, pitch – around lateral axis) will emerge with angular frequencies ω_ψ and ω_θ . Considering the propeller rotation, the primary system motion changes to the characteristic gyroscopic motion. The gyroscopic effect makes two independent mode shapes merge to rotational motion. The propeller axis makes an elliptical movement. The orientation of the propeller axis movement is backward relatively to the propeller rotation for the mode with lower frequency (backward whirl mode) and forward relatively to the propeller rotation for the mode with higher frequency (forward whirl mode). The mode shapes of gyroscopic modes are complex, since independent yaw and pitch modes have a phase

shift 90°. Condition of real mode shapes corresponds to the state of the undamped system.

The described gyroscopic mode shapes make harmonic changes of propeller blades angles of attack. They give rise to non-stationary aerodynamic forces, which may under the specific conditions induce a flutter. Possible states of the gyroscopic system from the flutter stability point of view for backward mode are explained in fig.2.

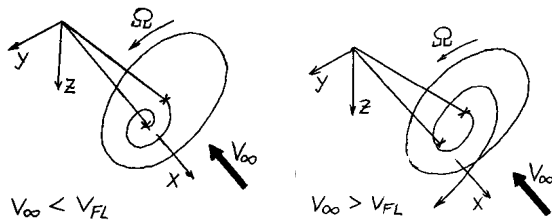


Fig.2. Stable and unstable state of gyroscopic vibrations for backward flutter mode

Provided that the air velocity is lower than critical value ($V_\infty < V_{FL}$), the system is stable and the motion is damped. If the airspeed exceeds the critical value ($V_\infty > V_{FL}$), the system becomes unstable and motion is diverging. The limit state ($V_\infty = V_{FL}$) with no total damping is called critical flutter state and V_{FL} is called critical flutter speed.

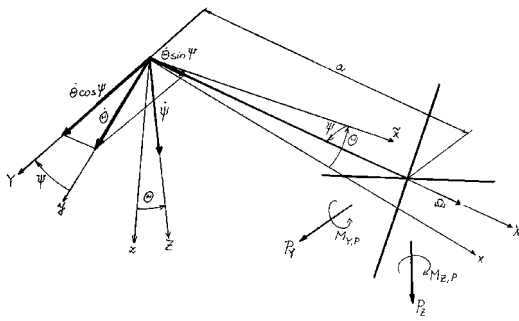


Fig.3. Kinematical scheme of the gyroscopic system

The basic problem of the analytical solution grounds on determination of the aerodynamic forces caused by the gyroscopic motion for propeller blades. The equations of motion were set up for system described in fig.1. The kinematical scheme including gyroscopic effects is shown in fig.3. The independent generalized coordinates are three angles (φ , Θ , Ψ). We assume the propeller angular velocity constant ($\varphi = \Omega t$), mass distribution symmetric

around X-axis and mass moments of inertia $J_Z \neq J_Y$.

Considering the small angles simplification, the equations of motion become:

$$\begin{aligned} J_Y \ddot{\Theta} + \frac{K_\Theta \gamma_\Theta}{\omega} \dot{\Theta} + J_X \Omega \dot{\Psi} + K_\Theta \Theta &= M_{Y,P} - a.P_Z \\ J_Y \ddot{\Psi} + \frac{K_\Psi \gamma_\Psi}{\omega} \dot{\Psi} - J_X \Omega \dot{\Theta} + K_\Psi \Psi &= M_{Z,P} + a.P_Y \end{aligned} \quad (1)$$

We formulate the propeller aerodynamic forces by means of the aerodynamic derivatives [1], [2] and make the simplification for the harmonic motion, then the final whirl flutter matrix equation will become:

$$\begin{aligned} \left(-\omega^2 [M] + j\omega \left([D] + [G] + q_\infty F_P \frac{D_P^2}{V_\infty} [D^A] \right) + \right. \\ \left. + \left([K] + q_\infty F_P D_P [K^A] \right) \right) \times \begin{bmatrix} \Theta \\ \Psi \end{bmatrix} = \{0\} \end{aligned} \quad (2)$$

The limit state emerges for the specific combination of parameters V_∞ and Ω , when the angular velocity ω is real. The whirl flutter characteristics are explained in fig.4, which describes influence of the propeller relative velocity ($V_\infty / (\Omega R)$) to the stability of undamped gyroscopic system. Increasing the propeller relative velocity makes increasing of the necessary stiffnesses K_Θ , K_Ψ . Also influences of the structural damping (stabilizing) and a distance propeller – mode shape node (destabilizing) are significant.

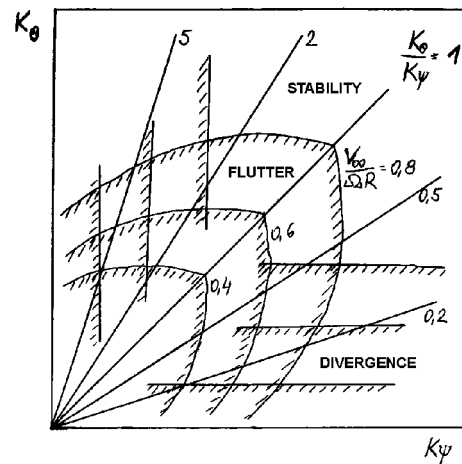


Fig.4. Influence of the propeller relative velocity ($V_\infty / (\Omega R)$) to the stability of undamped gyroscopic system

The whirl flutter appears at the gyroscopic rotational vibrations, the flutter frequency is the

same as the frequency of the backward gyroscopic mode. The critical state may be reached either due to increasing the air velocity or the propeller revolutions. Structural damping is a significant stabilization factor. On the contrary, the propeller pull force influence is barely noticeable. The most critical state is $K_{\Theta} = K_{\Psi}$, it means $\omega_{\Theta} = \omega_{\Psi}$ when the interaction of both independent motions is maximal. A special case of the eq.(2) for $\omega=0$ is the gyroscopic static divergence.

4 Ordinary Analysis Procedure

The whirl flutter solution by means of the NASTRAN program system grounds on the Strip Aerodynamic Theory for the propeller at the windmilling mode. A propeller is assumed rigid. For the rest structure is used a Wing – Body Interference Aerodynamic Theory. For a flutter stability solution there is used a PK method. The NASTRAN whirl flutter DMAP (Direct Matrix Abstraction Program) subroutine is supplemented by the external preprocessor (program propf.for) for calculation of the propeller aerodynamic matrices (formally damping and stiffness matrices) and optionally for calculation of the down / side wash effects.

The FE model can be prepared similarly as for the standard flutter analysis; the model must include the grid at the propeller center of gravity with propeller mass characteristics. Data for calculation of downwash and sidewash angles may be specified by means of the partitioning matrices. The first NASTRAN run calculates the down / side wash angles only. These data and other data concerning the engine and the propeller are inputs to the external preprocessor. Output data from preprocessor are added to the NASTRAN input, formally as a direct input to the stiffness and damping matrices. Partitioning matrices must be removed. The second NASTRAN run is the final one and makes a flutter stability calculation.

The propeller aerodynamic forces and moments are calculated by eq.(3):

$$P_Y = q_{\infty} F_p \left(c_{y\Psi} \Psi^* + c_{y\Theta} \Theta^* + c_{yq} \frac{\dot{\Theta}^* R}{V_{\infty}} \right)$$

$$\begin{aligned} P_Z &= q_{\infty} F_p \left(c_{z\Theta} \Theta^* + c_{z\Psi} \Psi^* + c_{zr} \frac{\dot{\Psi}^* R}{V_{\infty}} \right) \\ M_{Y,P} &= q_{\infty} F_p D_P \left(c_{m\Psi} \Psi^* + c_{mq} \frac{\dot{\Theta}^* R}{V_{\infty}} \right) \\ M_{Z,P} &= q_{\infty} F_p D_P \left(c_{n\Theta} \Theta^* + c_{nr} \frac{\dot{\Psi}^* R}{V_{\infty}} \right) \end{aligned} \quad (3)$$

Aerodynamic derivatives are given from propeller blade integrals [5], effective angles are shown in the fig.5.

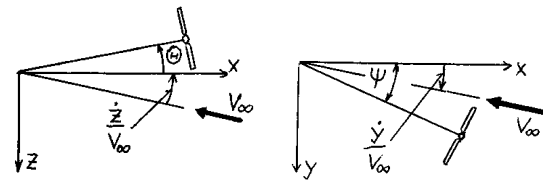


Fig.5. Effective static angles

An option to include the downwash and sidewash effects may be important for configuration with engines mounted to the wing. Downwash and sidewash angles behind the propeller describe interference between propeller and nacelle. Induced downwash and sidewash angles are added to the effective static angles (fig.5) by the eq.(4):

$$\begin{aligned} \Theta^* &= \Theta + \frac{\dot{z}}{V_{\infty}} - \frac{w_1}{V_{\infty}} \\ \Psi^* &= \Psi - \frac{\dot{y}}{V_{\infty}} + \frac{w_2}{V_{\infty}} \end{aligned} \quad (4)$$

Above mentioned induced down / side wash angles dependent on the reduced frequency can be obtained from the lift solution by partitioning the interference coefficients. The downwash effect influences only the aerodynamic stiffness matrix; influence to the aerodynamic damping matrix is neglected. Only interference between propeller and nacelle is included, interference between propeller and a wing is neglected.

5 Optimization Based Solution

The optimization is a process of the structure changes aimed to make an improvement considering determined conditions and parameters. Basically the optimization is a mathematical algorithm of seeking the optimal

parameters combination to minimize the objective function respecting the determined limitations and conditions.

Optimization procedures belong to the family of methods called “gradient-based”, since they determine the gradients of the objective function and constraints to determine a direction of searching for the optimum in the design space. Then it proceeds in that direction as far as they can go. After that it investigates if we are at the optimum point, if not the process is repeated until can make no more improvement of the objective without violating some constrain.

The optimization may cover various analyses types. For the static aeroelasticity, apart from the ordinary design responses like displacement, strain, stress, force, etc. the two specific types are applicable (trim variables and stability derivatives). For the flutter solution, the design response is represented by the total damping for a selected mode, air density, Mach number and velocity. Obviously synthetic responses defined as a function of other design responses, design variables, constants etc. are allowed. However, usage of such advanced applications assumes a knowledge regarding the flutter behavior of the structure.

For the optimization purposes, only the PK method is applicable. The basic flutter equation in modal coordinates is:

$$\left[M_{hh} p^2 + \left(B_{hh} - \frac{1}{4} \frac{\rho c V Q_{hh}^{Im}}{k} \right) p + \left(K_{hh} - \frac{1}{2} \rho V Q_{hh}^{Re} \right) \right] \{u_h\} = 0 \quad (5)$$

M_{hh} , B_{hh} and K_{hh} are modal mass, damping and stiffness matrices respectively. Aerodynamic loads are incorporated into damping and stiffness matrices. Aerodynamic matrices are dependent on the reduced frequency (k) at a gentle rate. All matrices are real; Q_{hh}^{Re} and Q_{hh}^{Im} are real and imaginary part of a complex aerodynamic matrix Q_{hh} . The decay rate coefficient is defined in connection with the complex eigenvalue:

$$p = \omega (\gamma \pm j) = p^{Re} + j p^{Im} \quad (6)$$

Flutter sensitivities are computed as rate of change of the transient decay coefficient γ with respect to changes in design variables ($\partial\gamma/\partial x_i$).

As mentioned, the most important parameters influencing the whirl flutter are the natural frequencies of the engine vertical and lateral vibration modes; and also a ratio of both ones. Let’s assume the inertia characteristics of the engine – propeller system and the residual structure reliably determined. That’s why the engine suspension stiffness parameters would be used as optimization parameters. We formulate two design variables: the rotational stiffness of the engine attachment around the vertical and lateral axes. Design properties and the relations to the design variables are to be defined in accordance with the stiffness model type (two springs, system of springs, beams, shells, combined model, etc.).

Design responses are specified particularly as a design constrains. They represent the demand to hold the selected frequency ratio and the whirl flutter stability below the selected certification speed as well. A frequency ratio is specified by the lower and upper bounds, the recommended interval bounds are $\pm(1 - 2)\%$. Demand of the flutter stability is realized through the damping value for the specific mode and speed. Considering the possible problems of the numeric solution, the flutter state damping of $g = 0$ is moved to a non-zero value, as described later. In the case of more than two degrees of freedom included in the solution, there is necessary to ensure also no other flutter instability below the certification speed. That’s why the latter constrain is extended also to the other mode shapes. The objective function is defined as minimization of the both frequencies sum.

During the problem solving, there were several different optimization approaches and options tested. The described solution has appeared as the best one, in particular, it is applicable also for the gyroscopic divergence.

Firstly, the target frequency ratio is set. One of the design variables is fixed at the nominal value; the other one is updated to reach the mentioned target ratio. For this purpose, usage

of the optimization solution for normal modes is appropriate. The objective function is defined as:

$$\min \left(\frac{\text{frequency}(2)}{\text{frequency}(1)} - \text{target ratio} \right) \quad (7)$$

This preparatory analysis provides the initial values of both design variables and the corresponding frequencies of both vertical and lateral engine vibration modes. The frequency ratio agrees with the target ratio as well. The next analysis is the main one. It is a composite solution of both normal modes and flutter optimization solution specified in the two separated subcases. The normal modes solution includes the design constrain of keeping the target ratio, defined as:

$$\frac{\text{frequency}(2)}{\text{frequency}(1)} = \text{target ratio} (\pm(1-2)\%) \quad (8)$$

Besides it includes the objective function, defined as:

$$\min (\text{frequency} (1) + \text{frequency} (2)) \quad (9)$$

The flutter solution includes the design constrain of the flutter stability ($g < 0$) below the certification speed. It is applied for all modes included in the analysis to prevent other type of the flutter instability apart from the whirl flutter below the certification speed. It is defined as:

$$\frac{g(V = V_{\text{certif.}}) - 0,03}{0,1} \in \langle -\infty; -0.3 \rangle \quad (10)$$

The flutter solution is performed just for the certification speed; input file must satisfy the specific whirl flutter analysis demands and include all the specific data, in particular data from the external preprocessor as described in the chapter 4. The NASTRAN whirl flutter DMAP subroutine must have been adapted for the NASTRAN optimization solver. The adapted subroutine is applicable for the NASTRAN v2005.0. The results from this main optimization analysis are the final design variables, and corresponding design properties values. The whirl flutter speed is equal to the certification speed; the frequency ratio of the vertical and lateral engine vibration frequencies is equal to the target ratio as well. The described procedure is also applicable for a case of

gyroscopic divergence, which may occur for the high target ratio values.

As a final phase, it is recommended to perform standard whirl flutter solution for standard number of velocities to check the flutter behavior of the updated structure. Described procedure is required to be repeated for the range of target frequency ratios, the order of the vertical and lateral modes (lower, higher) must be taken in account as well. It should be noted that in the most cases it is impossible to reach the values of frequency ratio extremely closed to the unity value due to the character of the stiffness model.

6 Application Examples

6.1 Aircraft Engine Component System

The first testing example represents a model of the flexibly attached isolated engine – propeller system of a small (10 seat) single nose-mounted turboprop aircraft (wingspan 13,8 m; length 12,2 m; max. take-of weight 3300 kg – see fig.6).

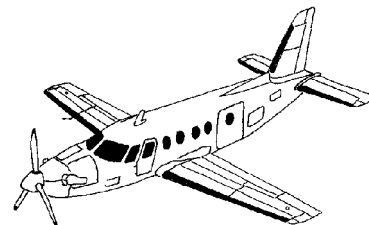


Fig. 6. Small transport aircraft

The FE model includes engine, propeller and engine bed inertia characteristics and the engine bed and engine mount isolators' stiffness characteristics as well. The engine – propeller inertia is modeled by means of concentrated masses with relevant moments of inertia. The flexibility of the mount isolators is modeled by means of two rotational springs placed at the node points of vertical and lateral engine vibrations mode shapes obtained from the ground vibration tests. The nominal stiffness of each spring was tuned to reach the natural frequencies from ground vibration tests as well. The described system was attached to the beam

model of the cantilevered engine bed.

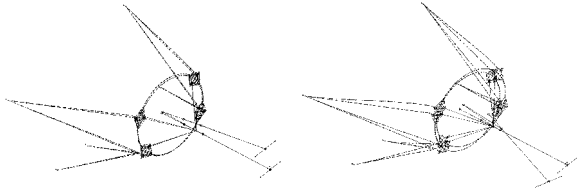


Fig. 7. Engine vibrations mode shapes (vertical - $f_0 = 10,43$ Hz; lateral - $f_0 = 14,84$ Hz)

There were two modes included in the flutter analysis, despite that the system has more degrees of freedom due to the beam engine bed model. Modes are listed in fig.7. Flutter analyses were performed for the aircraft aeroelastic certification altitude of $H = 2500$ m; certification speed for optimization was $1,2V_D = 150 \text{ m.s}^{-1}$ TAS. At first, the whirl flutter calculation for the nominal state was performed. There was no flutter state found. After that, the optimization analyses for selected frequency ratios were performed as described in the previous chapter. Analyses included both options of the modes order. The critical flutter frequency is maximal for the frequency ratio close to the unity value, for the high frequency ratios, the flutter transforms to divergence.

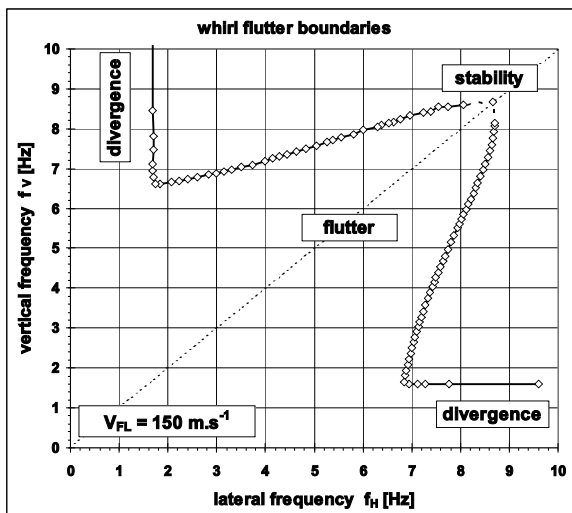


Fig. 8. Whirl flutter stability boundaries (critical values of natural frequencies)

Whirl flutter stability boundaries are presented in fig.8. Axes represent both vertical and lateral frequencies; the ratio value of unity was extrapolated. Whirl flutter frequencies are presented in fig.9. V-g-f diagram for the selected frequency ratio is presented in fig.10. For the evaluation of diagrams, it must be taken

into account, that there was a subsonic aerodynamic theory used, therefore the results for speed in the transonic or supersonic ranges doesn't represent the real state, but just artificial values.

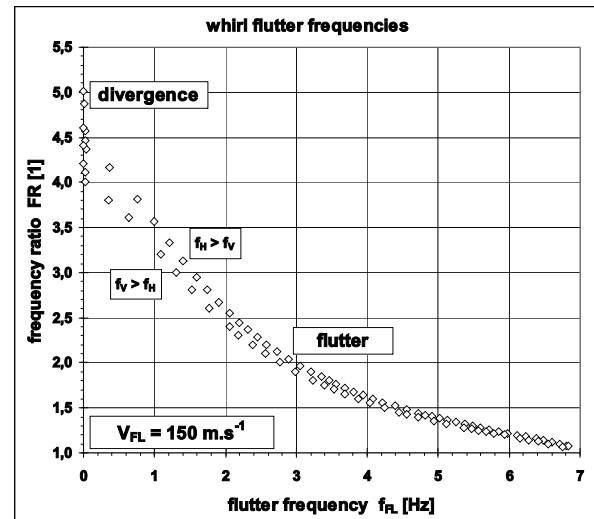


Fig. 9. Whirl flutter frequencies

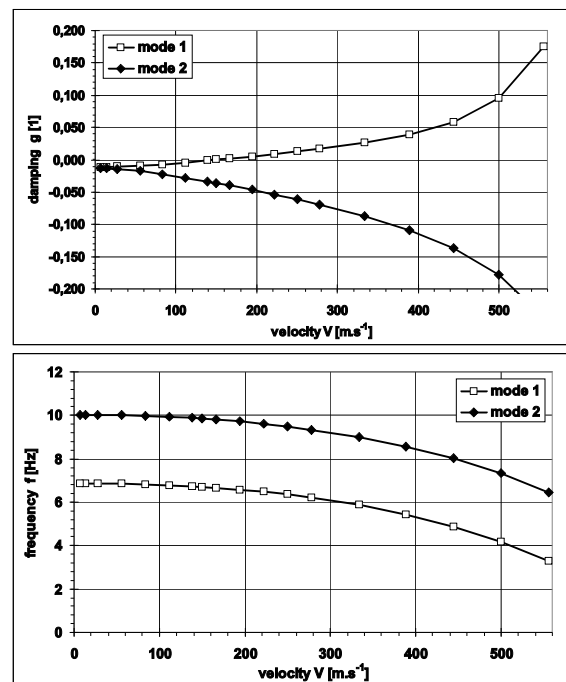


Fig. 10. V-g-f diagram (frequency ratio 1,098; $f_{FL} = 6,71$ Hz)

6.2 Aircraft Engine - Wing Component System

The second testing example represents a model of a cantilevered wing with a flexibly attached engine – propeller system of a twin wing-mounted engine 42 seat turboprop

commuter (wingspan 25,6 m; length 21,4 m; max. take-of weight 14500 kg – see fig.11).



Fig. 11. Twin-engine commuter

The FE model doesn't represent a full-scale aircraft, but the aeroelastic model with the length scale of 1/5 and the velocity scale of 1/6. The FE model (fig.12) includes engine, propeller and wing inertia characteristics and the engine mount isolators, engine bed and the wing stiffness characteristics as well. Character of the FE model corresponds to the hardware aeroelastic model. The engine – propeller and the wing inertias are modeled by means of concentrated masses with relevant moments of inertia. Flexibility of the engine attachment is modeled by springs. The two rotational springs simulate the engine bed flexibility in the vertical and lateral directions. Two further translational springs simulate the mount-isolators flexibility in pitch. The engine – propeller model is attached to the beam model of the cantilevered wing with an aileron.

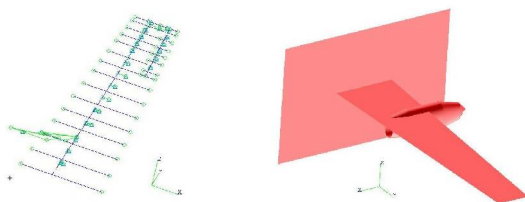


Fig. 12. FE model (structural, aerodynamic)

The model is prepared in a number of configurations concerning the fuel filling, stiffness of the aileron drive and the stiffness of the engine suspension. For the purpose of presented task, there was one specific configuration selected. Aerodynamic model consist of the wing – aileron and splitter Doublet – Lattice elements, the nacelle was modeled as a Slender and Interference Body. Interference effects were taken into account. An interconnection between structural and

aerodynamic part was realized via beam splines, the splitter was grounded by a surface spline.

Since on the full-scale aircraft, there is the

Tab.1. Modal characteristics summary

#	Title	f_0 [Hz]
1	1 st wing bending	3,094
2	Engine vertical vibration	3,791
3	Engine lateral vibration	4,628
4	1 st wing horizontal bending	8,353
5	2 nd wing bending	8,522
6	Aileron flapping	13,567
7	1 st wing torsion	16,591
8	2 nd wing bending	19,674
9	2 nd wing horizontal bending	22,407
10	2 nd wing bending	24,886

engine attached via mount isolators in two planes (engine bed ring and rear attachment), contrary to the previous example, the engine vibrations modes represent the vibrations of the engine bed. The modal characteristics of the selected configuration are listed in tab.1. Listed frequencies were compared with the experimental values obtained from the ground vibration test of the hardware model. An agreement between analytical and experimental results was assessed as satisfactory. As the

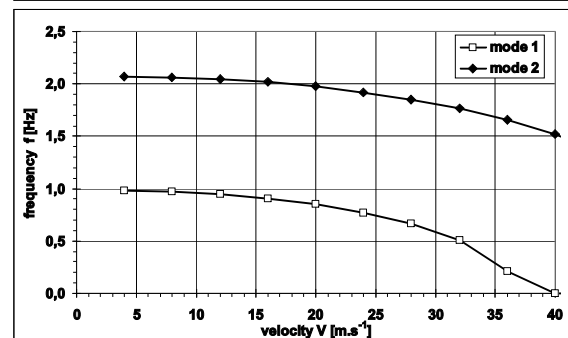
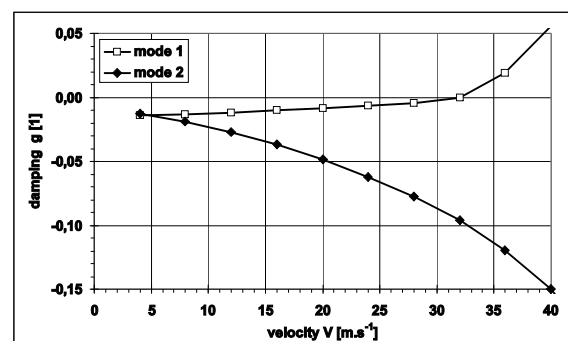


Fig. 13. V-g-f diagram – 2 modes (frequency ratio 1,652; $f_{FL} = 0,51$ Hz)

former example, firstly the whirl flutter calculation for a nominal state was performed. There was no whirl flutter instability found, just a wing bending – torsion – aileron flutter occurred ($V_{FL} = 68,5 \text{ m.s}^{-1}$; $f_{FL} = 12,2 \text{ Hz}$).

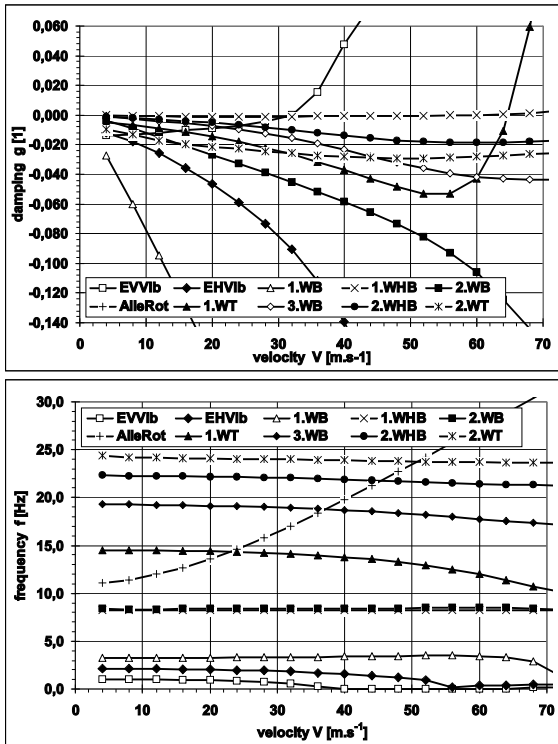


Fig. 14: V-g-f diagram – 10 modes (frequency ratio 1,653; $f_{FL} = 0,56 \text{ Hz}$)

Optimization based calculations were performed in the same way as have been already described in the previous example. The results look similar to those ones as well. A certification speed scaled down to the aeroelastic model scale was $1.2 \cdot V_D = 32 \text{ m.s}^{-1}$. Whirl flutter stability calculations were performed for subset of two modes (engine vertical and lateral vibrations) and for set of 10 modes listed in the tab.1 as well. Selected V-g-f diagram for the two and 10 modes calculations are presented in fig.13 and 14. There can be found a critical state at the velocity of 32 m.s^{-1} of the whirl flutter. Furthermore, in fig.14, there is the aileron flutter instability; it wasn't affected by the gyroscopic effect. Diagram for the 10 modes correspond to that one presented for the two modes calculation.

Whirl flutter stability boundaries are presented in fig.15. Axes represent both vertical and lateral frequencies; the value for the ratio of

unity was extrapolated. Stability boundaries for both two modes and 10 modes option are compared. The former case is more stable, it means, that remaining modes representing the flexibility of the wing have a slightly destabilizing effect. It gives reasons for demands to include the residual structure, particularly the wing elasticity to the whirl flutter analysis. This fact causes a considerable increasing of configurations for the whirl flutter analysis (fuel filling etc.). The presented procedure can be employed to assess the influences of such secondary parameters. Whirl flutter frequencies for the 10 modes solution are presented in the fig.16 as well.

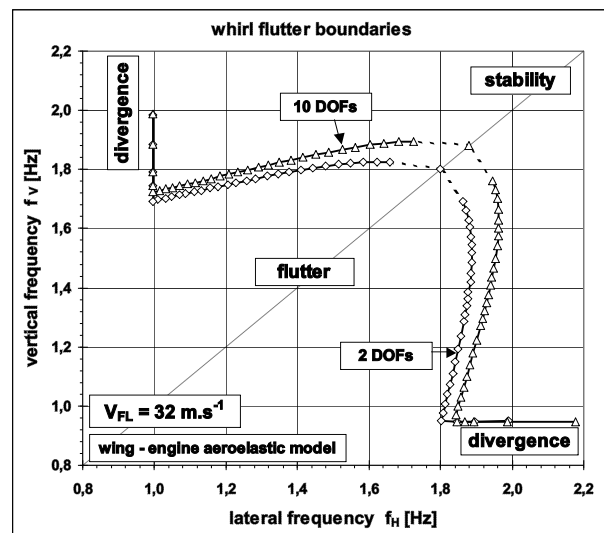


Fig. 15. Whirl flutter stability boundaries (critical values of natural frequencies)

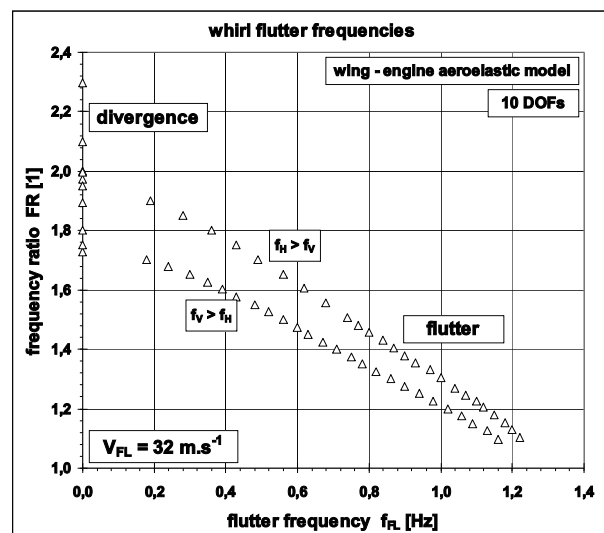


Fig. 16. Whirl flutter frequencies

7 Conclusion

Submitted paper presents a procedure for determination of the critical values of parameters regarding the whirl flutter stability. Parameters are stiffness of the engine suspension or engine vibration modes natural frequencies respectively. An optimization-based solution is employed. The procedure was tested on the two examples: the engine – propeller system of a single turboprop small transport aircraft and the engine – propeller – wing system of a twin turboprop commuter. The procedure replaces large parametric analytical studies varying the stiffness parameters by assessment of the critical values of them. It allows assessing easily influences of secondary parameters (residual structure of the aircraft). Furthermore it requires no experimental data from ground vibration tests, that's why it allows to move the whirl flutter analysis to the earlier phase of the aircraft development.

The procedure will be exploited during a new Czech EV-55 twin turboprop commuter aeroelastic certification.

8 Acknowledgement

The paper relates to the following research projects:

MSM 0001066903 “Research on Strength of Low-weight Structures with Special regard to Airplane Structures”;

6th FP EC Integrated Project „CESAR“ (Cost Effective Small Aircraft), Contract No.30888, Task 2.5 „Flutter Prevention for the Small Aircraft“.

References

- [1] Ribner, H.S.: *Propellers in Yaw*, NACA Report 820, 1945
- [2] Ribner, H.S.: *Formulas for Propellers in Yaw and charts of the Side – Force Derivatives*, NACA Report 819, 1945
- [3] Houbolt, J.C. – Reed, W.H.: Propeller – Nacelle Whirl Flutter, *Journal Aerospace Sciences*, Vol.29, pp.333 – 346, 1962

[4] Forsching, H.W.: *Grundlagen der Aeroelastik (translation: Osnovy Aerouprugosti)*, Mašinstroenie Moscow, IB 3112, 1984

[5] Rodden, W.P. – Rose, T.L.: Propeller / Nacelle Whirl Flutter Addition to MSC/NASTRAN, *Proceedings of the 1989 MSC World User's Conference*, Universal City, Ca.,U.S.A., Paper No.12, March 1989

[6] Čečrdle, J.: Výpočet vířivého flátru pomocí programového systému MSC.NASTRAN, *Journal Czech Aerospace Proceedings*, 4/2002, pp.26-30, ISSN 1211-877X, 2002

[7] Čečrdle, J.: Whirl Flutter Analysis of the Commuter Aircraft Aeroelastic Model Wing – Engine Component, *Proceedings of the Engineering Mechanics 2006, National Conference with International Participation*, 15.-18.5.2006, Svratka, Czech republic, paper no.119, book of extended abstracts pp. 42 – 43, full text on CD-ROM, ISBN 80-86246-27-2

[8] Čečrdle, J.: Whirl Flutter Analysis of the Small Transport Aircraft, *Proceedings of the IFASD 07 (International Forum on Aeroelasticity and Structural Dynamics)*, International Conference, Stockholm, Sweden, IF-021, CD-ROM

Copyright Statement

The authors confirm that they, and/or their company or institution, hold copyright on all of the original material included in their paper. They also confirm they have obtained permission, from the copyright holder of any third party material included in their paper, to publish it as part of their paper. The authors grant full permission for the publication and distribution of their paper as part of the ICAS2008 proceedings or as individual off-prints from the proceedings.